LEARNING TO SHARE IN MULTI-AGENT REINFORCEMENT LEARNING

Anonymous authors
Paper under double-blind review

ABSTRACT

In this paper, we study the problem of networked multi-agent reinforcement learning (MARL), where a number of agents are deployed as a partially connected network and each interacts only with nearby agents. Networked MARL requires all agents make decision in a decentralized manner to optimize a global objective with restricted communication between neighbors over the network. Inspired by the fact that *sharing* plays a key role in human's learning of cooperation, we propose LToS, a hierarchically decentralized MARL framework that enables agents to learn to dynamically share reward with neighbors so as to encourage agents to cooperate on the global objective. For each agent, the high-level policy learns how to share reward with neighbors to decompose the global objective, while the low-level policy learns to optimize local objective induced by the high-level policies in the neighborhood. The two policies form a bi-level optimization and learn alternately. We empirically demonstrate that LToS outperforms existing methods in both social dilemma and networked MARL scenario.

1 INTRODUCTION

In multi-agent reinforcement learning (MARL), there are multiple agents interacting with the environment via their joint action to cooperatively optimize an objective. Many methods of centralized training and decentralized execution (CTDE) have been proposed for cooperative MARL, such as COMA (Foerster et al., 2018), QMIX (Rashid et al., 2018), QPLEX (Wang et al., 2021), and FOP (Zhang et al., 2021). However, these methods suffer from the overgeneralization issue (Castellini et al., 2019). Moreover, they may not easily scale up with the number of agents due to centralized learning (Qu et al., 2020a).

In many MARL applications, there are a large number of agents that are deployed as a partially connected network and collaboratively make decisions to optimize the globally averaged return, such as communication networks (Kim et al., 2019) and traffic signal control (Wei et al., 2019). To deal with such scenarios, networked MARL is formulated to decompose the dependency among all agents into dependencies between only neighbors. To avoid decision-making with insufficient information, agents are permitted to exchange messages with neighbors over the network. In such settings, it is feasible for agents to learn to make decisions in a decentralized way (Zhang et al., 2018; Qu et al., 2020b). However, there are still difficulties of dependency if anyone attempts to make decision independently, *e.g., prisoner's dilemma* and *tragedy of the commons* (Pérolat et al., 2017). Existing methods tackle these problems by consensus update of value function (Zhang et al., 2018), credit assignment (Wang et al., 2020), or reward shaping (Chu et al., 2020). However, these methods rely on either access to global state and joint action (Zhang et al., 2018) or hand-crafted reward functions (Wang et al., 2020; Chu et al., 2020).

Inspired by the fact that *sharing* plays a key role in human's learning of cooperation (Eisenberg & Mussen, 1989), we propose *Learning To Share* (LToS), a hierarchically decentralized learning framework for networked MARL. LToS enables agents to learn to dynamically share reward with neighbors so as to collaboratively optimize the global objective. The high-level policies decompose the global objective into local ones by determining how to share their rewards, while the low-level policies optimize local objectives induced by the high-level policies. LToS learns in a decentralized manner, and we prove that the high-level policies are a mean-field approximation of the joint

high-level policy. Moreover, the high-level and low-level policies form a bi-level optimization and alternately learn to optimize the global objective.

LToS is a general hierarchical framework for networked MARL and can be easily realized by diverse combinations of RL algorithms. We currently implement LToS by DDPG (Lillicrap et al., 2016) as the high-level policy and DGN (Jiang et al., 2020) as the low-level policy. We empirically demonstrate that LToS outperforms existing methods for networked MARL in both social dilemma and networked MARL scenario.

2 Related Work

There are many recent studies for collaborative MARL. Most adopt CTDE (Foerster et al., 2018; Rashid et al., 2018; Wang et al., 2021; Zhang et al., 2021). Many of them are constructed on the basis of factorizing the joint Q-function (Rashid et al., 2018; Wang et al., 2021). However, these factorized methods suffer from the overgeneralization issue (Castellini et al., 2019). Other studies focus more on *decentralized training*, to which our work is more closely related, as summarized as follows.

Networked MARL. Zhang et al. (2018) and Qu et al. (2019) proposed consensus update of local value functions, where each agent keeps a local copy of the global value function but is assumed to have global information. Qu et al. (2020a) proposed intention propagation between agents, where each agent updates its policy based on intentions shared by other agents, but the policy may converge slowly due to propagated intentions over the network. Qu et al. (2020b) and Lin et al. (2020) investigated the exponential decay property, *i.e.*, the impact of agents on each other decays exponentially in their graph distance, while Chu et al. (2020) introduced a spatial discount factor to capture the influence between agents, which remains hand-tuned. However, none of these studies provide an explicit mechanism to solve social dilemma in networked MARL.

Reward Design. Hostallero et al. (2020) aimed at maximizing social welfare, but they simply used temporal difference error for reward shaping. As temporal difference error in deep RL hardly converges to zero, it still biases the optimization objective. Mguni et al. (2019) added an extra part to the original reward as non-potential based reward shaping and used Bayesian optimization to induce the convergence to a desirable equilibrium between agents. However, the extra part remains fixed during an episode, which makes it less capable of dealing with dynamic environments. Moreover, the reward shaping alters the original optimization problem. Hughes et al. (2018) proposed the inequity aversion model to balance agents' selfish desire and social fairness. Wang et al. (2020) considered learning the Shapley value as the credit assignment. However, these methods still rely on hand-crafted reward designs. Lupu & Precup (2020) added *gifting* as an extra action into the original MDP to modify the MDP and objective. Yang et al. (2020) proposed that each agent learns an incentive function and optimizes the policy in terms of both reward and incentives given by other agents. Obviously, both methods alter the original objective of optimization.

Unlike existing work, LToS enables agents to learn to dynamically share reward with other agents (without the bias of the optimization objective) such that they can collaboratively optimize the global objective in networked MARL.

3 Background

3.1 Networked Multi-Agent Reinforcement Learning

Assume N agents interact with an environment. Let $\mathcal{V} = \{1, 2, \cdots, N\}$ be the set of agents. The multi-agent system is modeled as an undirected graph $\mathcal{G}(\mathcal{V}, \mathcal{E})$, where each agent i serves as vertex i and $\mathcal{E} \subseteq \mathcal{V} \times \mathcal{V}$ is the set of all edges. Two agents $i, j \in \mathcal{V}$ can communicate with each other if and only if $e_{ij} = (i, j) \in \mathcal{E}$. We denote *agent i and its all neighbors in the graph together as a set* $\mathcal{N}_i$. The state of the environment $s \in \mathcal{S}$ transitions upon joint action $\boldsymbol{a} \in \mathcal{A}$ according to transition probability $\mathcal{P}_a : \mathcal{S} \times \mathcal{A} \times \mathcal{S} \to [0, 1]$, where joint action set $\mathcal{A} = \times_{i \in \mathcal{V}} \mathcal{A}_i$. Each agent i has a policy $\pi_i \in \Pi_i : \mathcal{S} \times \mathcal{A}_i \to [0, 1]$, and we denote the joint policy of all agents as $\boldsymbol{\pi} \in \Pi = \times_{i \in \mathcal{V}} \Pi_i$ (Zhang et al., 2018). For networked MARL, a common and realistic assumption is that the reward of each agent i just depends on its action and the actions of its neighbors (Qu et al., 2020a), *i.e.*,

$r_i(s, \boldsymbol{a}) = r_i(s, a_{\mathcal{N}_i})$. Moreover, each agent i may only obtain partial observation $o_i \in \mathcal{O}_i$, but can approximate the state by the observations of $\mathcal{N}_i$ (Jiang et al., 2020) or the observation history (Chu et al., 2020), which are all denoted by o_i for *simplicity*. The *global objective* is to maximize the sum of cumulative rewards of all agents , *i.e.*, $\sum_{t=0}^{\infty}\sum_{i=1}^{N}\gamma^t r_i^t$.

3.2 Markov Game

In such a setting, each agent could individually maximizes its own expected return, which is known as Markov game. This may lead to stable outcome or Nash equilibrium, which however is usually sub-optimal. Given $\boldsymbol{\pi}$, the value function of agent i is given by

$$v_i^{\boldsymbol{\pi}}(s) = \sum_{\boldsymbol{a}} \boldsymbol{\pi}(\boldsymbol{a}|s) \sum_{s'} p_a(s'|s, \boldsymbol{a})[r_i + \gamma v_i^{\boldsymbol{\pi}}(s')], \tag{1}$$

where $p_a \in \mathcal{P}_a$ describes the state transitions. A Nash equilibrium is defined as (Mguni et al., 2019)

$$v_i^{(\pi_i, \pi_{-i})}(s) \geq v_i^{(\pi_i', \pi_{-i})}(s), \quad \forall \pi_i' \in \Pi_i, \forall s \in \mathcal{S}, \forall i \in \mathcal{V},$$

where $\pi_{-i} = \times_{j \in \mathcal{V} \setminus \{i\}} \pi_j$.

4 Learning to Share in Multi-Agent Reinforcement Learning

LToS is a decentralized hierarchy. At each agent, the high-level policy determines the weights of reward sharing based on low-level policies while the low-level policy directly interacts with the environment to optimize local objective induced by the high-level policies. Therefore, they form a bi-level optimization and alternately learn towards the global objective.

4.1 Reward Sharing

The intuition of reward sharing is that if agents share their rewards with others, each agent has to consider the consequence of its actions on others, and thus it promotes cooperation. In networked MARL, as the reward of an agent is assumed to depend on the actions of neighbors, we allow reward sharing only between neighboring agents. This is because the change of actions of neighbors directly affects the reward while the agents outside the neighborhood can only affect the return of the agent indirectly by the change of state distribution. Moreover, this also fits the setting of networked MARL with restricted communication between neighbors.

For the graph of $\mathcal{V}$, we additionally define a set of directed edges, $\mathcal{D}$, constructed from $\mathcal{E}$. Specifically, we add a loop $d_{ii} \in \mathcal{D}$ for each agent i and split each undirected edge $e_{ij} \in \mathcal{E}$ into two directed edges: $d_{ij} = (i, j)$ and $d_{ji} = (j, i) \in \mathcal{D}$. Each agent i determines a weight $w_{ij} \in [0, 1]$ for each directed edge $d_{ij}, \forall j \in \mathcal{N}_i$, subject to the constraint $\sum_{j \in \mathcal{N}_i} w_{ij} = 1$, so that w_{ij} proportion of agent i's environment reward r_i will be shared to agent j. Let $\boldsymbol{w} \in \mathcal{W} = \times_{d_{ij} \in \mathcal{D}} w_{ij}$ be the weights of the graph. Therefore, the shaped reward after sharing for each agent i is defined as

$$r_i^{\boldsymbol{w}} = \sum_{j \in \mathcal{N}_i} w_{ji} r_j. \tag{2}$$

4.2 Hierarchy

Assume there is a joint high-level policy $\boldsymbol{\phi} \in \Phi : \mathcal{S} \times \mathcal{W} \to [0, 1]$ to determine $\boldsymbol{w}$. Given $\boldsymbol{\phi}$ and $\boldsymbol{w}$, we can define the value function of $\boldsymbol{\pi}$ at each agent i based on (1) as

$$\begin{aligned} v_i^{\boldsymbol{\pi}}(s; \boldsymbol{\phi}) &= \sum_{\boldsymbol{w}} \boldsymbol{\phi}(\boldsymbol{w}|s) \sum_{\boldsymbol{a}} \boldsymbol{\pi}(\boldsymbol{a}|s, \boldsymbol{w}) \sum_{s'} p_a(s'|s, \boldsymbol{a})[r_i^{\boldsymbol{w}} + \gamma v_i^{\boldsymbol{\pi}}(s'; \boldsymbol{\phi})], \\ v_i^{\boldsymbol{\pi}}(s; \boldsymbol{w}, \boldsymbol{\phi}) &= \sum_{\boldsymbol{a}} \boldsymbol{\pi}(\boldsymbol{a}|s, \boldsymbol{w}) \sum_{s'} p_a(s'|s, \boldsymbol{a})[r_i^{\boldsymbol{w}} + \gamma v_i^{\boldsymbol{\pi}}(s'; \boldsymbol{\phi})]. \end{aligned} \tag{3}$$

We express $\boldsymbol{w}$ as a discrete action for simplicity. It also holds for continuous action as long as we change all the summations to integrals. Let $V_{\mathcal{V}}^{\boldsymbol{\phi}}(s; \boldsymbol{\pi}) \doteq \sum_{i \in \mathcal{V}} v_i^{\boldsymbol{\pi}}(s; \boldsymbol{\phi})$ and $Q_{\mathcal{V}}^{\boldsymbol{\phi}}(s, \boldsymbol{w}; \boldsymbol{\pi}) \doteq \sum_{i \in \mathcal{V}} v_i^{\boldsymbol{\pi}}(s; \boldsymbol{w}, \boldsymbol{\phi})$.

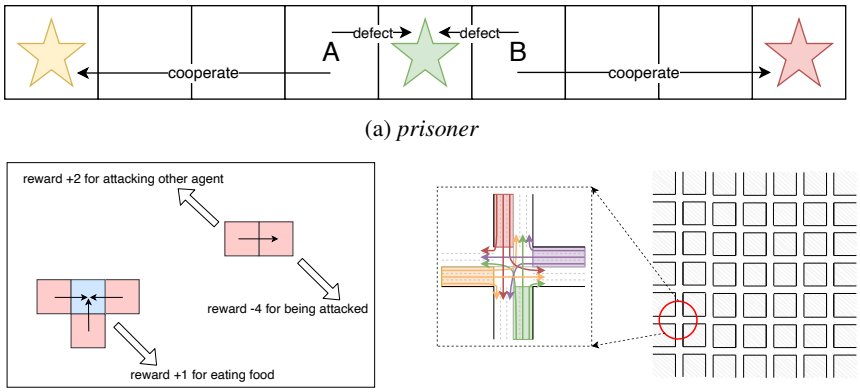

(a) *prisoner*

(b) *jungle*

(c) *traffic*

Figure 1: Three experimental scenarios: (a) *prisoner*, (b) *jungle*, and (c) *traffic*.

Proposition 1. *Given $\boldsymbol{\pi}$, $V_{\mathcal{V}}^{\boldsymbol{\phi}}(s;\boldsymbol{\pi})$ and $Q_{\mathcal{V}}^{\boldsymbol{\phi}}(s,\boldsymbol{w};\boldsymbol{\pi})$ are respectively the value function and action-value function of $\boldsymbol{\phi}$.*

Proof. The proof is deferred to Appendix. □

Proposition 1 implies that $\boldsymbol{\phi}$ directly optimizes the global objective by generating $\boldsymbol{w}$, given $\boldsymbol{\pi}$. Unlike existing hierarchical RL methods, we can directly construct the value function and action-value function of $\boldsymbol{\phi}$ based on the value function of $\boldsymbol{\pi}$ at each agent.

As $\boldsymbol{\phi}$ optimizes the global objective given $\boldsymbol{\pi}$ while π_i optimizes the shaped reward individually at each agent given $\boldsymbol{\phi}$ (assuming $\boldsymbol{\pi}$ convergent to Nash equilibrium or stable outcome, denoted as $\lim$), they form a bi-level optimization. Let $J_{\boldsymbol{\phi}}(\boldsymbol{\pi})$ and $J_{\boldsymbol{\pi}}(\boldsymbol{\phi})$ denote the objectives of $\boldsymbol{\phi}$ and $\boldsymbol{\pi}$ respectively. The bi-level optimization can be formulated as follows,

$$\begin{aligned} \max_{\boldsymbol{\phi}} \quad & J_{\boldsymbol{\phi}}(\boldsymbol{\pi}^*(\boldsymbol{\phi})) \\ s.t. \quad & \boldsymbol{\pi}^*(\boldsymbol{\phi}) = \arg\lim_{\boldsymbol{\pi}} J_{\boldsymbol{\pi}}(\boldsymbol{\phi}). \end{aligned} \tag{4}$$

4.3 Decentralized Learning

We start from collective learning to achieve global optimization of average reward. So far, the joint high-level policy is still in a centralized form. Note that the scenario needs a decentralized method and each agent has its own reward. Now we turn to learning the joint high-level policy in a decentralized way. The following proposition proves each agent's independence of each other on the high level.

Proposition 2. *The joint high level policy $\boldsymbol{\phi}$ can be learned in a decentralized manner, and the decentralized high-level policies of all agents form a mean-field approximation of $\boldsymbol{\phi}$.*

Proof. The proof is deferred to Appendix. □

Proposition 1 and 2 indicate that for each agent i, the low-level policy simply learns a local $\pi_i(a_i|s, w_i^{\text{in}})$, where $w_i^{\text{in}} = \{w_{ji} | j \in \mathcal{N}_i\}$, to optimize the cumulative reward of $r_i^{\boldsymbol{w}}$, since $r_i^{\boldsymbol{w}}$ is fully determined by w_i^{in} according to (2) and denoted as r_i^{w} from now on. And the high-level policy ϕ_i just needs to locally determine w_i^{out} to maximize the cumulative reward of $r_i^{\boldsymbol{\phi}}$ simplified as r_i^{ϕ}.

Therefore, for decentralized learning, (4) can be decomposed locally for each agent i as

$$\begin{aligned} \max_{\phi_i} \quad & J_{\phi_i}(\phi_{-i}, \pi_1^*(\boldsymbol{\phi}), \cdots, \pi_N^*(\boldsymbol{\phi})) \\ s.t. \quad & \pi_i^*(\boldsymbol{\phi}) = \arg\max_{\pi_i} J_{\pi_i}(\pi_{-i}, \phi_1(\boldsymbol{\pi}), \cdot\cdot, \phi_N(\boldsymbol{\pi})). \end{aligned} \tag{5}$$

Now we use max instead of lim because local policies can be compared and improved in a decentralized manner in a Markov game. We abuse the notation and let ϕ and π also denote their parameterizations respectively. To solve the optimization, we have

$$\begin{aligned}&\nabla_{\phi_i} J_{\phi_i}(\phi_{-i}, \pi_1^*(\boldsymbol{\phi}), \cdots, \pi_N^*(\boldsymbol{\phi})) \\ &\qquad \approx \nabla_{\phi_i} J_{\phi_i}(\phi_{-i}, \pi_1 + \alpha \nabla_{\pi_1} J_{\pi_1}(\boldsymbol{\phi}), \cdots, \pi_N + \alpha \nabla_{\pi_N} J_{\pi_N}(\boldsymbol{\phi})),\end{aligned} \tag{6}$$

where α is the learning rate for the low-level policy. Let π_i' denote $\pi_i + \alpha \nabla_{\pi_i} J_{\pi_i}(\boldsymbol{\phi})$, we have

$$\begin{aligned}&\nabla_{\phi_i} J_{\phi_i}(\phi_{-i}, \pi_1^*(\boldsymbol{\phi}), \cdots, \pi_N^*(\boldsymbol{\phi})) \\ &\qquad \approx \nabla_{\phi_i} J_{\phi_i}(\phi_{-i}, \pi_1', \cdots, \pi_N') + \alpha \sum_{j=1}^{N} \nabla^2_{\phi_i, \pi_j} J_{\pi_j}(\boldsymbol{\phi}) \nabla_{\pi_j'} J_{\phi_i}(\phi_{-i}, \pi_1', \cdots, \pi_N').\end{aligned}$$

The second-order derivative is neglected due to high computational complexity, without incurring significant performance drop such as in meta-learning (Finn et al., 2017). Similarly, we have

$$\begin{aligned}&\nabla_{\pi_i} J_{\pi_i}(\pi_{-i}, \phi_1^*(\boldsymbol{\pi}), \cdots, \phi_N^*(\boldsymbol{\pi})) \\ &\qquad \approx \nabla_{\pi_i} J_{\pi_i}(\pi_{-i}, \phi_1 + \beta \nabla_{\phi_1} J_{\phi_1}(\boldsymbol{\pi}), \cdots, \phi_N + \beta \nabla_{\phi_N} J_{\phi_N}(\boldsymbol{\pi})),\end{aligned}$$

where β is the learning rate of the high-level policy. Therefore, we can solve the bi-level optimization (4) by the first-order approximations in a decentralized way. For each agent i, ϕ_i and π_i are alternately updated.

In distributed learning, as each agent i usually does not have access to state, we further approximate $\phi_i(w_i^{\text{out}}|s)$ and $\pi_i(a_i|s, w_i^{\text{in}})$ by $\phi_i(w_i^{\text{out}}|o_i)$ and $\pi_i(a_i|o_i, w_i^{\text{in}})$, respectively. Moreover, in network MARL as each agent i is closely related to neighboring agents, (5) can be further seen as π_i maximizes the cumulative discounted reward of r_i^w given $\phi_{\mathcal{N}_i}$, where $\phi_{\mathcal{N}_i} = \times_{j \in \mathcal{N}_i} \phi_j$, and ϕ_i optimizes the cumulative discounted reward of r_i^w given $\pi_{\mathcal{N}_i}$ (*i.e.*, r_i^ϕ), where $\pi_{\mathcal{N}_i} = \times_{j \in \mathcal{N}_i} \pi_j$. During training, $\pi_{\mathcal{N}_i}$ and $\phi_{\mathcal{N}_i}$ are implicitly considered by interactions of w_i^{out} and w_i^{in} respectively. The architecture of LToS is illustrated in Figure 2. At each timestep, the high-level policy of each agent i makes a decision of action w_i^{out} as the weights of reward sharing based on the observation. Then, the low-level policy takes the observation and w_i^{in} as an input and outputs the action. Agent i obtains the shaped reward according to w_i^{in} for both the high-level and low-level policies. The gradients are backpropagated along purple dotted lines.

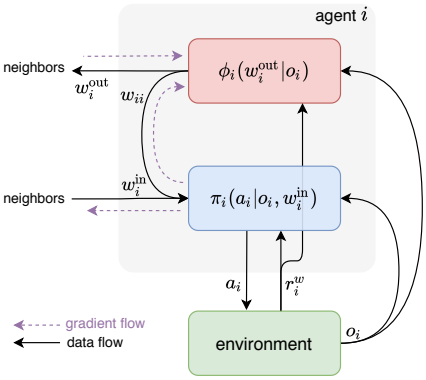

Figure 2: LToS

Further, from Proposition 1, we have: $q_i^{\phi_i}(s, w_i^{\text{out}}; \pi_{\mathcal{N}_i}) = v_i^{\pi_i}(s; w_i^{\text{in}}, \phi_{\mathcal{N}_i})$, where $q_i^{\phi_i}$ is the action-value function of ϕ_i given $\pi_{\mathcal{N}_i}$, $v_i^{\pi_i}$ is the value function of π_i given $\phi_{\mathcal{N}_i}$ and conditioned on w_i^{in}. As aforementioned, we approximately have $q_i^{\phi_i}(o_i, w_i^{\text{out}}) = v_i^{\pi_i}(o_i; w_i^{\text{in}})$. We can see that the action-value function of ϕ_i is equivalent to the value function of π_i. That said, we can use a single network to approximate these two functions simultaneously. For a deterministic low-level policy, the high-level and low-level policies can share a same action-value function. In the current instantiation of LToS, we use DGN (Jiang et al., 2020) (Q-learning) for the low-level policy and DDPG (Lillicrap et al., 2016) for the high-level policy. Thus, the Q-network of DGN also serves as the critic of DDPG, and the gradient of w_i^{in} is calculated based on the maximum Q-value of a_i.

For completeness, Algorithm 1 (see Appendix B) gives the training procedure of LToS based on DDPG and DGN. More discussions about training LToS are also available in Appendix C.

5 EXPERIMENTS

For the experiments, we adopt three scenarios *prisoner*, *jungle*, and *traffic* depicted in Figure 1, where *prisoner* and *jungle* (Jiang et al., 2020) are grid games about social dilemma that easily measures agents' cooperation, while *traffic* is a realistic scenario of networked MARL. We obey

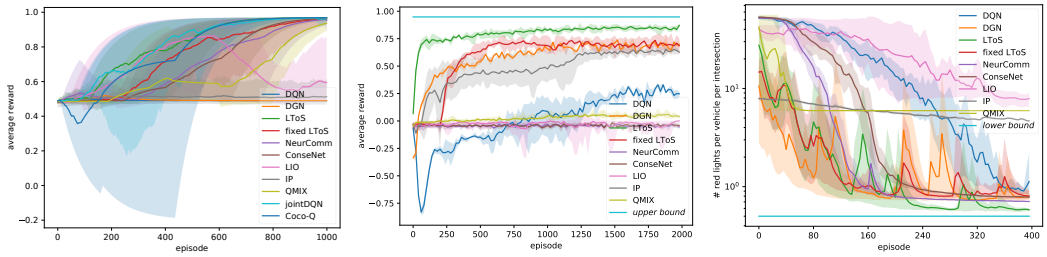

(a) *prisoner* (b) *jungle* (c) *traffic*

Figure 3: Learning curves in (a) *prisoner*, (b) *jungle*, and (c) *traffic*. All the curves are plotted using 5 training runs with different random seeds, where the solid line is the mean and the shadowed area is enclosed by the min and max value.

the principle of networked MARL that only allows communication in neighborhood as Zhang et al. (2018) and Chu et al. (2020).

To illustrate the reward sharing scheme each agent learned, we use a simple indicator: *selfishness*, the reward proportion that an agent chooses to keep for itself. For ablation, we keep the sharing weights fixed for each agent, named *fixed* LToS. Throughout the experiments, we additionally compare with the baselines including DQN and DGN, where DGN also serves the ablation of LToS without reward sharing as DGN is the low-level policy of LToS. To maximize the global return directly by centralized learning, we use QMIX (Rashid et al., 2018) as a baseline throughout the three scenarios and two other ones in *prisoner*. Moreover, as LToS aims to bring a harmonious cooperation by reward sharing in networked MARL, we compared LToS to three methods for networked MARL, *i.e.*, ConseNet (Zhang et al., 2018), NeurComm (Chu et al., 2020) and Intention Propagation (abbreviated as IP) (Qu et al., 2020a), and LIO (Yang et al., 2020) for incentivized learning, all of which use recurrent neural network (RNN) or graph neural network (GNN) for the partially observable environment. More details of hyperparameters are available in Appendix D.

5.1 PRISONER

We use *prisoner*, a grid game version of the well-known matrix game *prisoner's dilemma* from Sodomka et al. (2013) to empirically demonstrate that LToS is able to learn cooperative policies to achieve the global optimum (*i.e.*, maximize globally averaged return). As illustrated in Figure 1a, there are two agents A and B that respectively start on two sides of the middle of a grid corridor with *full* observation. At each timestep, each agent chooses an action *left* or *right* and moves to the corresponding adjacent grid, and every action incurs a cost -0.01. There are three goals, two goals at both ends and one in the middle. The agent gets a reward $+1$ for reaching the goal. The game ends once some agent reaches a goal or two agents reach different goals simultaneously. This game resembles prisoner's dilemma: going for the middle goal ("defect") will bring more rewards than the farther one on its side ("cooperate"), but if two agents both adopt that, a collision occurs and only one of the agents wins the goal with equal probability. On the contrary, both agents obtain a higher return if they both "cooperate", though it takes more steps. The highest possible return is 1.

Figure 3a illustrates the learning curves of all the methods in terms of average return. Note that for all three scenarios, we present the average of 5 training runs with different random seeds by solid lines and the min/max value by shadowed areas. As a result of self-interest optimization, DQN converges to the "defect/defect" Nash equilibrium where each agent receives an expected reward about 0.5. So does DGN since it only aims to take advantage of its neighbors' observations while *prisoner* is a fully observable environment already. Given a hand-tuned reward shaping factor to direct agents to maximize average return, NeurComm and *fixed* LToS agents are able to cooperate eventually. So are ConseNet and QMIX. However, they converge slowly. In contrast, IP agents learn at a slower pace and its performance is only a little higher than 0.5. LIO agents cooperate soon enough at the beginning, but they cannot form steady cooperation and perhaps need longer training to get rid of such instability.

JointDQN, Coco-Q (Sodomka et al., 2013), and LToS perform similarly and outperform other methods. JointDQN is one centralized DQN that takes control of joint actions of both agent A and B, and thus should be able to achieve the best performance but still takes time to converge even in such

a simple two-agent scenario. As a modified tabular Q-learning method, Coco-Q introduces the coco value (Kalai & Kalai, 2010) as a substitute for the expected return in the Bellman equation and regards the difference as transferred reward. However, it is specifically designed for some games, and it is hard to be extended beyond two-player games. LToS can learn the reward sharing scheme where one agent at first gives all the reward to the other so that both of them are prevented from "defect", and thus achieve the best average return quickly, as observed in the experiment. By *prisoner*, we verify that LToS can escape from local optimum by learning to share reward.

5.2 JUNGLE

Jungle is a scenario about moral dilemma proposed by Jiang et al. (2020) . As illustrated in Figure 1b, there are N agents and L stationary foods. At each timestep, each agent can attack or move to one adjacent grid. Eating (attacking food) brings a positive reward $+1$, but attacking other agents obtains a higher reward $+2$. The victim, however, suffers a negative reward -4, which makes each attack between agents a negative-sum action. Moreover, attacking a blank grid gets a small negative reward -0.01 (inhibiting excessive attacks). We follow the original setting of Jiang et al. (2020): map size = 30×30 grids, $N = 20$, $L = 12$, and the observation consists of one's coordinates and a field of 11×11 grids nearby. Each agent has 3 closest agents as its neighbors. Compared to *prisoner*, *jungle* has much more agents, and thus JointDQN and Coco-Q are disregarded for this scenario. Another challenge is that the network topology is dynamic since each agent can always move. Fortunately, the topology change slowly and predictably, and algorithms may get the time-varying neighbor set $\mathcal{N}_i$ as part of the input. Therefore, it is still likely to estimate the shaped rewards and value functions well.

Table 1: Average reward per step of all the methods in *jungle*.

DQN	DGN	*fixed* LToS	**LToS**	NeurComm	ConseNet	LIO	IP	QMIX	upper bound
0.24	0.66	0.71	**0.86**	-0.05	-0.04	0.00	0.63	0.04	0.95

Figure 3b illustrates the learning curves of all the methods, and their performance after convergence is also summarized in Table 1. NeurComm, ConseNet and QMIX do not perform well in this task. In NeurComm, each agent gets a "delayed global information". However, a stable pattern of delayed global information cannot be formed when the communication is conducted via a dynamic topology. ConseNet is constructed on the basis of a premise of *full observation*, and it can hardly learn well when the input is not only partial but also fairly varying in sequence and content. LIO agents also perform badly, since they cannot be distinguished from one another in the dynamic topology and thus fail to learn a proper incentive function. Moreover, LIO requires opponent modeling, but it is hard to simultaneously model all other agents in a dynamic environment. QMIX is free from these problems. While aiming at global optimization, like LIO, it realizes that attacking usually means a negative-sum action, but as a result, it avoids attacking as well as eating most of the time and thus only achieves a reward slightly higher than 0. Another possible reason to explain the performance QMIX is its scalability. As there are 20 agents in the scenario, it can be hard to learn the joint action-value function to directly optimize the average return (Qu et al., 2020a). Also, we can see that a fixed reward sharing scheme does not bring any gain over DGN. This is because fixed reward sharing does not adapt to the dynamic topology. By learning proper reward sharing and adjusting to changing circumstances, LToS outperforms all other baselines. Note that there is an upper bound for average reward per step for *jungle*. By estimating the average distance between each agent and the food that is the closest to it at the beginning of one episode, we can give a loose upper bound around 0.95 to reflect our improvement. The experimental results in *jungle* verify that LToS can also adapts to considerably varying topology in networked MARL.

In Appendix E.1, we illustrate the representative behaviors of agents learned by difference methods, and we compare LToS and ablation baselines with different number of agents to verify the scalability of LToS. As a result, LToS can always achieve the best performance as the agent population size increases.

5.3 TRAFFIC

In *traffic*, as illustrated in Figure 1c , we aim to investigate the capability of LToS in dealing with highly dynamic environment through reward sharing. We adopt the same problem setting as Wei et al. (2019). In a road network, each agent serves as traffic signal control at an intersection. The observation of an agent consists of a one-hot representation of its current phase (directions for red/green lights) and the number of vehicles on each incoming lane of the intersection. At each timestep, an agent chooses a phase from the pre-defined phase set for the next time interval, *i.e.*, 10 seconds. The reward is set to be the negative of the sum of the queue lengths of all approaching lanes at current timestep. The global objective is to minimize average wait time of all vehicles in the road network, which is equivalent to minimizing the sum of queue lengths of all intersections over an episode (Zheng et al., 2019). The experiment was conducted on a traffic simulator, CityFlow (Zhang et al., 2019). We use a 6×6 grid network with 36 intersections (agents). The traffic flows were generated to simulate dynamic traffic flows including both peak and off-peak period, and the statistics is summarized in Table 2.

Table 2: Statistics of traffic flows

Time (second)	Arrival Rate (vehicles/s)
$0 - 600$	1
$600 - 1,200$	$1/4$
$1,200 - 1,800$	$1/3$
$1,800 - 2,400$	2
$2,400 - 3,000$	$1/5$
$3,000 - 3,600$	$1/2$

For better demonstration, we choose to show the normalized metric of wait time: the average number of red lights one vehicle waits for at per intersection, and we can give an unrealistic loose lower bound 0.50 to reflect our improvement. Figure 3c shows the learning curves of all the methods in terms of that in logarithmic form. The performance after convergence is summarized in Table 3, where LToS outperforms all other methods. LToS outperforms DGN, which demonstrates the reward sharing scheme learned by the high-level policy indeed helps to improve the cooperation of agents. Without the high-level policy, *i.e.*, given fixed sharing weights, *fixed* LToS does not perform well in dynamic environment. This indicates the necessity of the high-level policy. The performance of IP agents increases so slowly that they cannot converge efficiently. Although NeurComm and ConseNet both take advantage of RNN for partially observable environments, LToS still outperforms these methods, which verifies the great improvement of LToS in networked MARL. QMIX is confined to suboptimality (Mahajan et al., 2019). As observed in the experiment, QMIX tries to release traffic flows from one direction while stopping flows from the other direction all the time, because this will only make two rows of intersections on the border blocked but keep most of the intersections from any traffic jam all the time. However, the global optimality actually does not need to be constructed on the sacrifice of anyone. Some similar thing happens to LIO. It is likely because LIO contains some sensitive parameters (Yang et al., 2020) and agents are hard to learn and coordinate their incentive functions since the original reward functions change acutely once an improper operation causes traffic congestion. An introduction of some explicit coordination mechanism may also alleviate the problem, like that of NeurComm and ConseNet.

The experimental results in *traffic* verify that LToS can also handle highly dynamic environment in networked MARL. Additionally, we visualize the variation of *selfishness* of all agents during an episode in Appendix E.2.

Table 3: Average number of red lights one vehicle waits for at per intersection of all the models in *traffic*

DQN	DGN	*fixed* LToS	**LToS**	NeurComm	ConseNet	LIO	IP	QMIX	lower bound
0.90	0.78	0.80	**0.58**	0.71	0.78	7.74	4.67	5.94	0.50

6 Conclusion

In this paper, we proposed LToS, a hierarchically decentralized framework for networked MARL. LToS enables agents to share reward with neighbors so as to encourage agents to cooperate on the global objective. For each agent, the high-level policy learns how to share reward with neighbors to decompose the global objective, while the low-level policy learns to optimize local objective induced by the high-level policies in the neighborhood. Experimentally, we demonstrate that LToS outperforms existing methods in both social dilemma and networked MARL scenario.

REFERENCES

Jacopo Castellini, Frans A Oliehoek, Rahul Savani, and Shimon Whiteson. The representational capacity of action-value networks for multi-agent reinforcement learning. In *AAMAS*, 2019.

Tianshu Chu, Sandeep Chinchali, and Sachin Katti. Multi-agent reinforcement learning for networked system control. In *ICLR*, 2020.

Nancy Eisenberg and Paul Henry Mussen. *The roots of prosocial behavior in children*. Cambridge University Press, 1989.

Chelsea Finn, Pieter Abbeel, and Sergey Levine. Model-agnostic meta-learning for fast adaptation of deep networks. In *ICML*, 2017.

Jakob Foerster, Gregory Farquhar, Triantafyllos Afouras, Nantas Nardelli, and Shimon Whiteson. Counterfactual multi-agent policy gradients. In *AAAI*, 2018.

J. M. Hammersley and P. Clifford. Markov fields on finite graphs and lattices. *unpublished manuscript*, 1971.

David Earl Hostallero, Daewoo Kim, Sangwoo Moon, Kyunghwan Son, Wan Ju Kang, and Yung Yi. Inducing cooperation through reward reshaping based on peer evaluations in deep multi-agent reinforcement learning. In *AAMAS*, 2020.

Edward Hughes, Joel Z. Leibo, Matthew G. Phillips, Karl Tuyls, Edgar A. Duéñez-Guzmán, Antonio García Castañeda, Iain Dunning, Tina Zhu, Kevin R. McKee, Raphael Koster, Heather Roff, and Thore Graepel. Inequity aversion improves cooperation in intertemporal social dilemmas. In *NeurIPS*, 2018.

Jiechuan Jiang, Chen Dun, Tiejun Huang, and Zongqing Lu. Graph convolutional reinforcement learning. In *ICLR*, 2020.

Adam Tauman Kalai and Ehud Kalai. Cooperation and competition in strategic games with private information. In *EC*, 2010.

Daewoo Kim, Sangwoo Moon, David Hostallero, Wan Ju Kang, Taeyoung Lee, Kyunghwan Son, and Yung Yi. Learning to schedule communication in multi-agent reinforcement learning. In *ICLR*, 2019.

Timothy P. Lillicrap, Jonathan J. Hunt, Alexander Pritzel, Nicolas Heess, Tom Erez, Yuval Tassa, David Silver, and Daan Wierstra. Continuous control with deep reinforcement learning. In *ICLR*, 2016.

Yiheng Lin, Guannan Qu, Longbo Huang, and Adam Wierman. Multi-agent reinforcement learning in time-varying networked systems, 2020.

Andrei Lupu and Doina Precup. Gifting in multi-agent reinforcement learning. In *AAMAS*, 2020.

Anuj Mahajan, Tabish Rashid, Mikayel Samvelyan, and Shimon Whiteson. Maven: Multi-agent variational exploration. In *NeurIPS*, 2019.

David Mguni, Joel Jennings, Emilio Sison, Sergio Valcarcel Macua, Sofia Ceppi, and Enrique Munoz de Cote. Coordinating the crowd: Inducing desirable equilibria in non-cooperative systems. In *AAMAS*, 2019.

Julien Pérolat, Joel Z Leibo, Vinicius Zambaldi, Charles Beattie, Karl Tuyls, and Thore Graepel. A multi-agent reinforcement learning model of common-pool resource appropriation. In *NeurIPS*, 2017.

Chao Qu, Shie Mannor, Huan Xu, Yuan Qi, Le Song, and Junwu Xiong. Value propagation for decentralized networked deep multi-agent reinforcement learning. In *NeurIPS*, 2019.

Chao Qu, Hui Li, Chang Liu, Junwu Xiong, James Zhang, Wei Chu, Yuan Qi, and Le Song. Intention propagation for multi-agent reinforcement learning. *arXiv:2004.08883*, 2020a.

Guannan Qu, Yiheng Lin, Adam Wierman, and Na Li. Scalable multi-agent reinforcement learning for networked systems with average reward. In *NeurIPS*, 2020b.

Tabish Rashid, Mikayel Samvelyan, Christian Schroeder, Gregory Farquhar, Jakob Foerster, and Shimon Whiteson. Qmix: Monotonic value function factorisation for deep multi-agent reinforcement learning. In *ICML*, 2018.

Eric Sodomka, Elizabeth Hilliard, Michael Littman, and Amy Greenwald. Coco-q: Learning in stochastic games with side payments. In *ICML*, 2013.

Jianhao Wang, Zhizhou Ren, Terry Liu, Yang Yu, and Chongjie Zhang. Qplex: Duplex dueling multi-agent q-learning. In *ICLR*, 2021.

Jianhong Wang, Yuan Zhang, Tae-Kyun Kim, and Yunjie Gu. Shapley q-value: A local reward approach to solve global reward games. In *AAAI*, 2020.

Hua Wei, Nan Xu, Huichu Zhang, Guanjie Zheng, Xinshi Zang, Chacha Chen, Weinan Zhang, Yanmin Zhu, Kai Xu, and Zhenhui Li. Colight: Learning network-level cooperation for traffic signal control. In *CIKM*, 2019.

Jiachen Yang, Ang Li, Mehrdad Farajtabar, Peter Sunehag, Edward Hughes, and Hongyuan Zha. Learning to incentivize other learning agents. In *NeurIPS*, 2020.

Huichu Zhang, Siyuan Feng, Chang Liu, Yaoyao Ding, Yichen Zhu, Zihan Zhou, Weinan Zhang, Yong Yu, Haiming Jin, and Zhenhui Li. Cityflow: A multi-agent reinforcement learning environment for large scale city traffic scenario. In *WWW*, 2019.

Kaiqing Zhang, Zhuoran Yang, Han Liu, Tong Zhang, and Tamer Başar. Fully decentralized multi-agent reinforcement learning with networked agents. In *ICML*, 2018.

Tianhao Zhang, Yueheng Li, Chen Wang, Guangming Xie, and Zongqing Lu. Fop: Factorizing optimal joint policy of maximum-entropy multi-agent reinforcement learning. In *ICML*, 2021.

Guanjie Zheng, Xinshi Zang, Nan Xu, Hua Wei, Zhengyao Yu, Vikash Gayah, Kai Xu, and Zhenhui Li. Diagnosing reinforcement learning for traffic signal control. *arXiv:1905.04716*, 2019.

A PROOFS

A.1 PROOF OF PROPOSITION 1

Proof. Let $r_i^{\boldsymbol{\phi}} \doteq \sum_{\boldsymbol{a}} \boldsymbol{\pi}(\boldsymbol{a}|s,\boldsymbol{w}) r_i^{\boldsymbol{w}}$ and $p_w(s'|s,\boldsymbol{w}) \doteq \sum_{\boldsymbol{a}} \boldsymbol{\pi}(\boldsymbol{a}|s,\boldsymbol{w}) p_a(s'|s,\boldsymbol{a})$. As commonly assumed the reward is deterministic given s and $\boldsymbol{a}$, from (3), we have,

$$\begin{aligned} v_i^{\boldsymbol{\pi}}(s;\boldsymbol{\phi}) &= \sum_{\boldsymbol{w}} \boldsymbol{\phi}(\boldsymbol{w}|s) \sum_{\boldsymbol{a}} \boldsymbol{\pi}(\boldsymbol{a}|s,\boldsymbol{w})[r_i^{\boldsymbol{w}} + \sum_{s'} p_a(s'|s,\boldsymbol{a})\gamma v_i^{\boldsymbol{\pi}}(s';\boldsymbol{\phi})] \\ &= \sum_{\boldsymbol{w}} \boldsymbol{\phi}(\boldsymbol{w}|s) \sum_{s'} p_w(s'|s,\boldsymbol{w})[r_i^{\boldsymbol{\phi}} + \gamma v_i^{\boldsymbol{\pi}}(s';\boldsymbol{\phi})], \end{aligned} \tag{7}$$

where $p_w \in \mathcal{P}_w : \mathcal{S} \times \mathcal{W} \times \mathcal{S} \to [0,1]$ describes the state transitions given $\boldsymbol{\pi}$.

Let $r_{\mathcal{V}}^{\boldsymbol{\phi}} \doteq \sum_{i\in\mathcal{V}} r_i^{\boldsymbol{\phi}}$, and from (7) we have

$$\begin{aligned} V_{\mathcal{V}}^{\boldsymbol{\phi}}(s;\boldsymbol{\pi}) &= \sum_{i\in\mathcal{V}} \sum_{\boldsymbol{w}} \boldsymbol{\phi}(\boldsymbol{w}|s) \sum_{s'} p_w(s'|s,\boldsymbol{w})[r_i^{\boldsymbol{\phi}} + \gamma v_i^{\boldsymbol{\pi}}(s';\boldsymbol{\phi})] \\ &= \sum_{\boldsymbol{w}} \boldsymbol{\phi}(\boldsymbol{w}|s) \sum_{s'} p_w(s'|s,\boldsymbol{w})[\sum_{i\in\mathcal{V}} r_i^{\boldsymbol{\phi}} + \gamma \sum_{i\in\mathcal{V}} v_i^{\boldsymbol{\pi}}(s';\boldsymbol{\phi})] \\ &= \sum_{\boldsymbol{w}} \boldsymbol{\phi}(\boldsymbol{w}|s) \sum_{s'} p_w(s'|s,\boldsymbol{w})[r_{\mathcal{V}}^{\boldsymbol{\phi}} + \gamma V_{\mathcal{V}}^{\boldsymbol{\phi}}(s';\boldsymbol{\pi})], \end{aligned}$$

and similarly,

$$\begin{aligned} Q_{\mathcal{V}}^{\boldsymbol{\phi}}(s,\boldsymbol{w};\boldsymbol{\pi}) &= \sum_{i\in\mathcal{V}} \sum_{s'} p_w(s'|s,\boldsymbol{w})[r_i^{\boldsymbol{\phi}} + \gamma \sum_{\boldsymbol{w}'} \phi(\boldsymbol{w}'|s') v_i^{\boldsymbol{\pi}}(s';\boldsymbol{w}',\boldsymbol{\phi})] \\ &= \sum_{s'} p_w(s'|s,\boldsymbol{w})[r_{\mathcal{V}}^{\boldsymbol{\phi}} + \gamma \sum_{\boldsymbol{w}'} \boldsymbol{\phi}(\boldsymbol{w}'|s') Q_{\mathcal{V}}^{\boldsymbol{\phi}}(s',\boldsymbol{w}';\boldsymbol{\pi})]. \end{aligned}$$

Moreover, from the definitions of $r_i^{\boldsymbol{w}}$ and $r_i^{\boldsymbol{\phi}}$ we have

$$\begin{aligned} r_{\mathcal{V}}^{\boldsymbol{\phi}} &= \sum_{\boldsymbol{a}} \boldsymbol{\pi}(\boldsymbol{a}|s,\boldsymbol{w}) \sum_{i\in\mathcal{V}} r_i^{\boldsymbol{w}} \\ &= \sum_{\boldsymbol{a}} \boldsymbol{\pi}(\boldsymbol{a}|s,\boldsymbol{w}) \sum_{i\in\mathcal{V}} \sum_{j\in\mathcal{N}_i} w_{ji} r_j \\ &= \sum_{\boldsymbol{a}} \boldsymbol{\pi}(\boldsymbol{a}|s,\boldsymbol{w}) \sum_{(i,j)\in\mathcal{D}} w_{ij} r_i = \sum_{\boldsymbol{a}} \boldsymbol{\pi}(\boldsymbol{a}|s,\boldsymbol{w}) \sum_{i\in\mathcal{V}} r_i. \end{aligned}$$

Thus, given $\boldsymbol{\pi}$, $V_{\mathcal{V}}^{\boldsymbol{\phi}}(s)$ and $Q_{\mathcal{V}}^{\boldsymbol{\phi}}(s,\boldsymbol{w})$ are respectively the value function and action-value function of $\boldsymbol{\phi}$ in terms of the sum of expected cumulative rewards of all agents, *i.e.*, the global objective. □

A.2 PROOF OF PROPOSITION 2

First, we introduce one definition and one lemma.

Definition 1 (**Markov Random Field**). *A Markov Random Field (MRF) is a graph $\mathcal{G} = (\mathcal{V}, \mathcal{E})$ that satisfies:*

$$P(X_i|\{X_j\}_{j\in\mathcal{V}\setminus\{i\}}) = P(X_i|\{X_j\}_{j\in\mathcal{N}_i}) \tag{8}$$

where X_i is some random variable associated with node $i, \forall i \in \mathcal{V}$.

Lemma 1 (**Hammersley–Clifford Theorem**). *A probability distribution that has a strictly positive mass or density satisfies one of the Markov properties with respect to an undirected graph $\mathcal{G}$ if and only if it is a Gibbs random field, i.e., its density can be factorized over the cliques (or complete subgraphs) of the graph. (Hammersley & Clifford, 1971)*

Now we begin the proof of Proposition 2.

Proof. Let $d_{ij} \in \mathcal{D}$ serve as a vertex with action w_{ij} and reward $w_{ij}r_i$ in a new graph $\mathcal{G}'$. Each vertex has its own local policy $\phi_{ij}(w_{ij}|s)$. Note that in the sense of mean-field approximation, we focus on neighbors and find a MRF: each w_{ij} needs and only needs to be determined considering other $\{w_{ik}\}_{k\in\mathcal{N}_i\setminus\{j\}}$, because their actions are subject to the constraint $\sum_{j\in\mathcal{N}_i} w_{ij} = 1$. It accords with the adjacency relationship in $\mathcal{G}'$. According to Lemma 1, it is also a Gibbs random field.

Now we consider the cliques that we factor $\boldsymbol{\phi}(\boldsymbol{w}|s)$ over. For $\forall i \in \mathcal{V}$, $\{d_{ij}|j \in \mathcal{N}_i\}$ should form a complete subgraph in $\mathcal{G}'$. As $d_{ij} \in \mathcal{G}'$ only connects to $\{d_{ik}|k \in \mathcal{N}_i\setminus\{j\}\}$, the complete subgraph is also a maximal clique. Therefore, we have $\boldsymbol{\phi}(\boldsymbol{w}|s) \approx \prod_{i\in\mathcal{V}} \phi_i(w_i^{\text{out}}|s)$, where $w_i^{\text{out}} = \{w_{ij}|j \in \mathcal{N}_i\}$. Note that technically each agent i can determine $\{w_{ij}|j \in \mathcal{N}_i\}$ simultaneously. We allow agent i to take charge of $\phi_i(w_i^{\text{out}}|s)$ as its high-level policy which is a joint policy of the complete subgraph in $\mathcal{G}'$, so that we can turn the view back to $\mathcal{G}$ from $\mathcal{G}'$ and verify each agent's independence in the high level. □

This proposition gives a factorization which is different from existing studies. First, our factorization differs from $\pi(\boldsymbol{a}|s) = \Pi_{i=1}^{N}\pi(a_i|s)$ (Zhang et al., 2018), since each agent needs to make decision considering other agents' plan. Also in contrast to Qu et al. (2020a), they parameterize intention propagation by GNN and other neural networks to factorize the joint policy thoroughly, while we accept incomplete factorization and group indecomposable cliques by each agent to form high-level policies that are also decentralized and independent of each other.

B ALGORITHM

We describe LToS as Algorithm 1.

Algorithm 1 LToS

Initialize ϕ_i parameterized by θ_i and π_i parameterized by μ_i for each agent i (ϕ_i is learned by DDPG and π_i is learned by DGN, and they share the Q-network)
for $t = 0$ to T **do**
  for each agent i **do**
    exchange observations and get o_i
    $w_i^{\text{out}} \leftarrow \phi_i(o_i)$ with exploration
    exchange w_i^{out} and get w_i^{in}
    $a_i \leftarrow \pi_i(o_i; w_i^{\text{in}})$ with exploration
    execute a_i, obtain r_i, and transition to $o_i' = o_{i,t+1}$
    exchange r_i and get r_i^w
    store $(o_i, w_i^{\text{in}}, a_i, r_i^w, o_i', \mathcal{N}_i)$ in $\mathcal{B}_i$
  end for
  if $t \bmod update_frequency$ **then**
    for each agent i **do**
      sample a minibatch from replay buffer $\mathcal{B}_i$: $D = \{(o_i, w_i^{\text{in}}, a_i, r_i^{\boldsymbol{w}}, o_i', \mathcal{N}_i)\}$
      exchange $w_i^{\text{out}'} \leftarrow \phi_i'(o_i')$ and get $w_i^{\text{in}'}$
      set $y_i \leftarrow r_i^{\boldsymbol{w}} + \gamma q_i^{\pi_i'}(o_i', a_i'; w_i^{\text{in}'})|_{a_i'=\pi_i'(o_i'; w_i^{\text{in}'})}$
      update μ_i by $\nabla_{\mu_i}\mathbb{E}_D(y_i - q_i^{\pi_i}(o_i, a_i; w_i^{\text{in}}))^2$
      exchange $w_i^{\text{out}} \leftarrow \phi_i(o_i)$ and get w_i^{in}
      compute $g_i^{\text{in}} = \nabla_{w_i^{\text{in}}} q_i^{\pi_i}(o_i, \arg\max_{a_i} q_i^{\pi_i}; w_i^{\text{in}})$
      exchange g_i^{in} and get gradient g_i^{out} for w_i^{out}
      update θ_i by $\frac{1}{|D|}\sum_{o_i\in D}(\nabla_{\theta_i}\phi_i(o_i))^{\mathsf{T}} g_i^{\text{out}}$
      softly update target networkrs θ_i' and μ_i'
    end for
  end if
end for

C DISCUSSIONS ON TRAINING LTOS

As a hierarchically decentralized MARL framework, LToS brings some challenges for training.

Selfishness Initializer. On the basis of a straightforward idea that one should generally focus more on its own reward than that of others when optimizing its own policy, the initial output of each high-level policy network is supposed to be higher on the sharing weight of its own than others. We choose to predetermine the initial selfishness to learn the high-level policy effectively. However, with normal initializers, the output of the high-level policy network will be evenly distributed initially. Therefore, we use a special *selfishness initializer* for each high-level policy network instead. As we use the softmax to produce the weights, which guarantees the constraint: $\sum_{j \in \mathcal{N}_i} w_{ij} = 1, \forall i \in \mathcal{V}$, we specially set the bias of the last fully-connected layer so that each decentralized high-level policy network tends to keep for itself the same reward proportion as the given selfishness initially. The rest of reward is still evenly distributed among neighbors. LToS learns started from such initial weights, while *fixed* LToS uses such weights throughout each experiment. Moreover, we use grid search to find the best selfishness for *fixed* LToS in *traffic* and *jungle*. For *prisoner* we deliberately set the selfishness to 0.5 so that *fixed* LToS directly optimizes the average return.

Unified Pseudo Random Number Generator. LToS is learned in a decentralized manner. This incurs some difficulty for experience replay. As each agent i needs w_i^{in} to update network weights for both high-level and low-level policies, it should sample from its buffer a batch of experiences where each sampled experience should be synchronized across the batches of all agents (*i.e.*, the experiences should be collected at a same timestep). To handle this, all agents can simply use a unified pseudo random number generator and the same random seed.

Different Time Scales. As many hierarchical RL methods do, we can set the high-level policy to running at a slower time scale than the low-level one. Proposition 1 still holds if we expand $v_i^{\boldsymbol{\pi}}$ for more than one step forward. Assuming the high-level policy runs every M timesteps, we can fix $w_i^{\text{out}} = w^{\text{out},t+1} = \cdots = w^{\text{out},t+M-1}$. M is referred to as *action interval* in Table 5.

Infrequent Parameter Update with Small Learning Rate. Based on the continuity of $\boldsymbol{w}$, a small modification of $\boldsymbol{\phi}$ means a slight modification of local reward functions, and will intuitively result in an equally slight modification of the low-level value functions. This guarantees the low-level policies are highly reusable.

Unordered Output. Essentially, the output of high-level policy network is unordered and has a one-to-one match with each neighbor as input. The output of deep neural network, however, is generally ordered and has trouble in varying with the input order. To settle this, we take advantage of DGN which is insensitive of neighbor order as input. Besides, we modify the structure to make the output keep consistency with the neighbor part of input in the relative order.

D HYPERPARAMATERS

As three experimental scenarios are quite different, we may use different hyperparameters. Note that we also tuned the hyparameters for the baselines with grid search. Table 4 summarizes the hyperparameters of DQN, DGN that also serves as the low-level network of LToS, and IP. We choose the setting of original DGN in *jungle* while the setting of Wei et al. (2019) in *traffic* for consistency. Table 5 summarizes the hyperparameters of the high-level network of LToS, which are different from the low-level network. Table 6 summarizes the hyperparameters of NeurComm and ConseNet, which adhere to the implementation (Chu et al., 2020). In addition, for tabular Coco-Q, the step-size parameter is 0.5, and for IP, the regularizer factor is 0.2. We adopt soft update for both high-level and low-level networks and use an Ornstein-Uhlenbeck Process (abbreviated as OU) for high-level exploration.

Both *fixed* LToS and NeurComm exploit static reward shaping, but they adopt different reward shaping schemes which are hard to compare directly. We consider a simple indicator: Self Neighbor Ratio (SNR), the ratio of reward proportion that an agent chooses to keep for itself to that it obtains from a single neighbor. As the rest reward is evenly shared with neighbors in LToS, for each agent i, we have $\text{SNR} = {}^{\text{selfishness}}/_{\text{1-selfishness}} \times (|\mathcal{N}_i| - 1)$ for LToS, and $\text{SNR} = {}^{1}/_{\alpha}$ for NeurComm where α is the spatial discount factor. We adjust the initial selfishness and α to set the SNR of both methods at the same level for fair comparison.

Table 4: Hyperparameters for DQN, DGN (also serves as the low-level policy network of LToS), and IP

Hyperparamater	*Prisoner*	*Jungle*	*Traffic*
sample size	10	10	1,000
batch size	10	10	20
buffer capacity	200,000	200,000	10,000
$\epsilon_{start}, \epsilon_{decay}, \epsilon_{end}$	0.8/1/0.8	0.6/0.996/0.01	0.4/0.9/0.05
initializer	random normal	random normal	random normal
optimizer	Adam	Adam	RMSProp
learning rate	1e-3	1e-4	1e-3
γ	0.99	0.96	0.8
τ for soft update	0.1	0.01	0.1
# MLP units	32 & 32	512 & 128	32 & 32
MLP activation	ReLU	ReLU	ReLU
# encoder MLP layers	2	2	2
# attention heads for DGN	4	4	1

Table 5: Hyperparameters for the high-level policy network of LToS

Hyperparamater	*Prisoner*	*Jungle*	*Traffic*
update frequency	1 step	100 episodes	5 episodes
action interval	1 step	1 step	15 steps
sample size	2,000	5,000	1,000
batch size	32	32	20
noise for exploration	ϵ + Gaussian	OU	OU
noise parameter	$\epsilon = 0.8, \sigma = 1$	$\sigma = 0.025\epsilon$	$\sigma = 0.25\epsilon$
initializer	selfishness	selfishness	selfishness
initial selfishness	0.5	0.5	0.8
optimizer	SGD	SGD	SGD
learning rate	1e-1	1e-4	1e-3
last MLP layer activation	softmax	softmax	softmax

Table 6: Hyperparameters for NeurComm, ConseNet, LIO and QMIX

Hyperparamater	*Prisoner*	*Jungle*	*Traffic*
initializer	orthogonal	orthogonal	orthogonal
optimizer	RMSProp	RMSProp	RMSProp
learning rate	5e-3	5e-5	5e-4
# MLP units	20	512 & 128	16
MLP activation	ReLU	ReLU	ReLU
# cell state units	20	512	16
# hidden state units	20	512	16
RNN type for NeurComm and ConseNet	LSTM	LSTM	LSTM
RNN type for QMIX	GRU	GRU	GRU
hypernetwork layer1 units for QMIX	2×20	20×512	36×16
hypernetwork layer2 units for QMIX	20	512	16
α for NeurComm	1	0.33	0.1
$\epsilon_{start}, \epsilon_{decay}, \epsilon_{end}$ for LIO	0.8/0.99/0.01	0.6/0.996/0.01	0.2/0.9/0.01
α_θ for LIO	1	1e-4	1e-4
R_{max} for LIO	2	3	0.1

E VISUALIZATION

E.1 JUNGLE

Figure 4 illustrates the representative behaviors of agents learned by difference methods. For NeurComm, ConseNet (and the same with LIO), most agents are not even close to the foods, so as to avoid being attacked. Even though, there are still conflict and sneak attack between agents some-

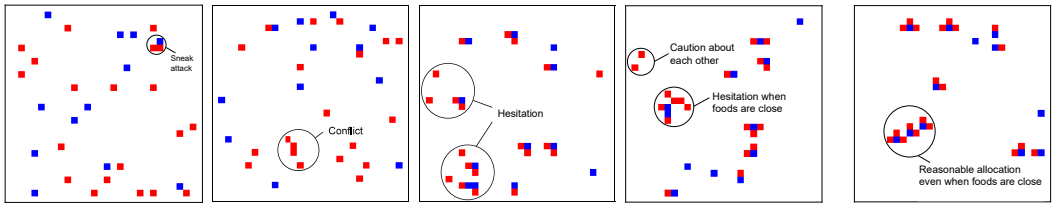

(a) NeurComm (b) ConseNet (c) IP (d) DGN (e) LToS

Figure 4: Representative behaviors of agents learned by (a) NeurComm, (b) ConseNet, (c) IP, (d) DGN, and (e) LToS in *jungle*.

times. IP and DGN agents learn much better, but agents may still be cautious about each other, which leads to hesitation when they are near the same food. LToS agents learn to properly share the food even if the foods are close (*i.e.*, agents are easy to be attacked) as depicted in Figure 4e and demonstrate much better cooperation than the agents learned by other methods.

# agents	DGN	*fixed* LToS	**LToS**	*upper bound*
10	0.52	0.63	**0.71**	0.93
20	0.66	0.71	**0.86**	0.95
30	0.77	0.79	**0.88**	0.96
40	0.84	0.80	**0.90**	0.96
50	0.86	0.79	**0.91**	0.97

(a) Statistics of performance

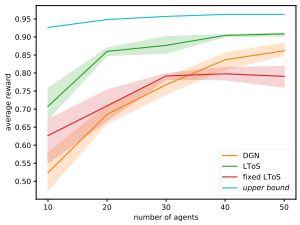

(b) Line graph of performance

Figure 5: Average reward per step of methods in *jungle* with different number of agents

Besides, we compared LToS and ablation baselines (*i.e.*, DGN and *fixed* LToS) with different number of agents (*i.e.*, from 10 to 50). All the setting remains the same except that the number of agents and food grows proportionally (*i.e.*, $\#agents/\#foods = 5/3$). As depicted in Figure 5b, LToS can always achieve the best performance as the agent population size increases.

E.2 TRAFFIC

We visualize the variation of *selfishness* of all agents during an episode in *traffic* in Figure 6a and 6b. Figure 6a depicts the temporal variance of selfishness for each agent. For most agents, there are two valleys occurred exactly during two peak periods (*i.e.*, $0-600$s and $1,800-2,400$s). This is because for heavy traffic agents need to cooperate more closely, which can be induced by being less selfish. We can see this from the fact that selfishness is even lower in the second valley where the traffic is even heavier (*i.e.*, 2 *vs.* 1 vehicles/s). Therefore, this demonstrates that the agents learn to adjust their extent of cooperation to deal with dynamic environment by controlling the sharing weights. Figure 6b shows the spatial pattern of selfishness at different timesteps, where the distribution of agents is the same as the road network in Figure 1c. The edge and inner agents tend to have very different selfishness. In addition, inner agents keep their selfishness more uniform during off-peak periods, while they diverge and present cross-like patterns during peak periods. This shows that handling heavier traffic requires more diverse reward sharing schemes among agents to promote more sophisticated cooperation.

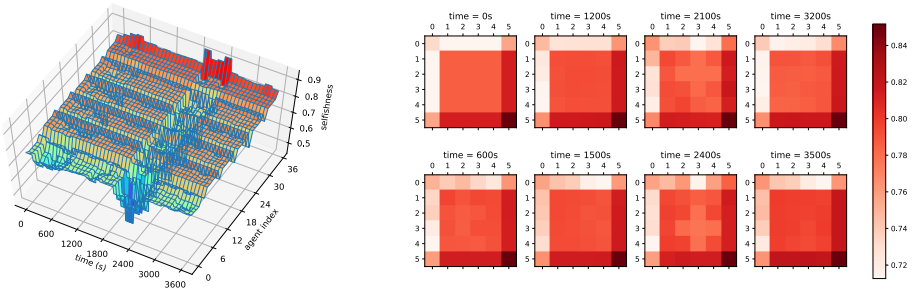

(a) temporal pattern

(b) spatial pattern

Figure 6: Patterns of *selfishness* in *traffic*.